Biogeosciences Discuss., 12, 6783–6820, 2015
www.biogeosciences-discuss.net/12/6783/2015/
doi:10.5194/bgd-12-6783-2015
© Author(s) 2015. CC Attribution 3.0 License.

Biogeosciences Discussions
Open Access

This discussion paper is/has been under review for the journal Biogeosciences (BG).
Please refer to the corresponding final paper in BG if available.

Energy balance closure on a winter wheat stand: comparing the eddy covariance technique with the soil water balance method

K. Imukova, J. Ingwersen, M. Hevart, and T. Streck

Institute of Soil Science and Land Evaluation, University of Hohenheim, 70593 Stuttgart, Germany

Received: 26 March 2015 – Accepted: 13 April 2015 – Published: 6 May 2015

Correspondence to: K. Imukova (kristina.imukova@uni-hohenheim.de)

Published by Copernicus Publications on behalf of the European Geosciences Union.

Abstract

The energy balance of eddy covariance (EC) flux data is typically not closed. The nature of the gap is usually not known, which hampers using EC data to parameterize and test models. The present study elucidates the nature of the energy gap of EC flux data from winter wheat stands in southwest Germany. During the vegetation periods 2012 and 2013, we continuously measured, in a half-hourly resolution, latent (LE) and sensible (H) heat fluxes using the EC technique. Measured fluxes were adjusted with either the Bowen-ratio (BR), H or LE post-closure method. The adjusted LE fluxes were tested against evapotranspiration data (ET_{WB}) calculated using the soil water balance (WB) method. At sixteen locations within the footprint of an EC station, the soil water storage term was determined by measuring the soil water content down to a soil depth of 1.5 m. In the second year, the volumetric soil water content was also continuously measured in 15 min resolution in 10 cm intervals down to 90 cm depth with sixteen capacitance soil moisture sensors. During the 2012 vegetation period, the H post-closed LE flux data ($ET_{EC} = 3.4 \pm 0.6$ mm day^{-1}) corresponded closest with the result of the WB method (3.3 ± 0.3 mm day^{-1}). ET_{EC} adjusted by the BR (4.1 ± 0.6 mm day^{-1}) or LE (4.9 ± 0.9 mm day^{-1}) post-closure method were higher than the ET_{WB} by 20 and 33 %, respectively. In 2013, ET_{WB} was in best agreement with ET_{EC} adjusted with the H post-closure method during the periods with low amount of rain and seepage. During these periods the BR and LE post-closure methods overestimated ET by about 30 and 40 %, respectively. During a period with high and frequent rainfalls, ET_{WB} was in-between ET_{EC} adjusted by H and BR post-closure methods. We conclude that, at most vegetation periods on our site, LE is not a major component of the energy balance gap. Our results indicate that the energy balance gap other energy fluxes and unconsidered or biased energy storage terms.

BGD
12, 6783–6820, 2015

Energy balance closure on a winter wheat stand

K. Imukova et al.

1 Introduction

The eddy covariance (EC) method is a widely used, long-standing method to directly measure turbulent energy and matter fluxes near the land surface. As a quality check, the energy balance closure (EBC) of eddy covariance flux measurements may be computed. According to the first law of thermodynamics, energy must be conserved. At the land surface, the surface energy budget equation, written here for its major components, must be fulfilled:

$$R_\mathrm{n} = \mathrm{LE} + H + G \tag{1}$$

Here, R_n ($\mathrm{W\,m^{-2}}$) is net radiation, and LE ($\mathrm{W\,m^{-2}}$) and H ($\mathrm{W\,m^{-2}}$) denote the latent heat and sensible heat flux, respectively. The symbol G ($\mathrm{W\,m^{-2}}$) stands for ground heat flux. Minor flux terms such as energy storage in the canopy or energy conversion by photosynthesis are generally neglected (see e.g. Leuning et al., 2012). In several studies, minor energy fluxes were carefully investigated as potential sources for the imbalance, and the general finding from these studies is that considering these minor terms helps to improve the EBC (Jacobs et al., 2008; Lamaud et al., 2001; Meyers and Hollinger, 2004; Oncley and Foken et al., 2007).

Usually the sum of the two turbulent fluxes measured with the EC method is systematically lower than the so-called available energy ($R_\mathrm{n} - G$). As a consequence, the energy balance at the Earth's surface usually cannot be closed with the EC technique. The quotient of turbulent fluxes and available energy expresses the energy balance closure:

$$\mathrm{EBC} = \frac{(H + \mathrm{LE})}{(R_\mathrm{n} - G)} \tag{2}$$

In general, EBC ranges between 70 to 90 % as observed over different types of surface ranging from bare soil to a forest (Oncley et al., 2007; Wilson et al., 2002; Twine et al., 2000). Low EBCs (60–80 %) were mainly observed at various agricultural sites

BGD
12, 6783–6820, 2015

CC BY

and bare soil, whereas over forest they were typically higher (80–90 %) (Charuchittipan et al., 2014; Wilson et al., 2002; Foken, 2008a; Panin et al., 2008; Stoy et al., 2013). The imbalance usually occurs during day time, particularly around noon, whereas at night at low fluxes EBC is often close to unity (Oncley et al., 2007). It was long thought that the energy balance gap originates from the instrumental errors of the EC-measurements. However, the accuracy of the energy flux measurements and data quality has significantly increased during last years. According to Foken (2008a), measuring errors cannot explain the problem of the imbalance provided that measurements and data processing were performed carefully. In a more recent paper, Foken (2010) investigated the EBC of the LITFASS-2003 experimental data. He concluded that the observed lack of EBC on the local scale in heterogeneous landscape can be explained only by deficits in measurement concepts and methodologies. This conclusion is supported by Heusinkveld (2004), who found a perfect EBC over a homogeneous surface: a desert in Israel. Tsvang (1991) and Stoy (2013) also discussed that the heterogeneities of the surrounding area are an important factor contributing to the lack of EBC. Large eddies can be formed at the boundary of areas with different land use (Foken, 2008a). Large eddies do not touch the land surface, their transport of heat, water or gas is not detected by the EC station. Mauder et al. (2007) performed airborne flux measurements over a boreal ecosystem in Canada in order to measure large eddy fluxes which cannot be captured by a single EC station. They found that these fluxes were in the same order of magnitude as energy balance residuals observed at EC stations close to the flight track. However, this large eddy theory has not been fully embraced by the scientific community. Leuning (2012), for instance, evaluated EBC of the La Thuile dataset. He concluded that unrealistically large and positive horizontal gradients in temperature and humidity would be needed for advective flux divergences in order to explain the EBC problem at half-hourly time scale. Other potential reasons for the imbalance discussed in the literature relate to the possible loss of low- and/or high-frequency components (Wolf et al., 2007; Sakai et al., 2001; Barr et al., 1994). A small fraction of the energy balance gap may also be explained by energy storage in the canopy and photosyn-

BGD
12, 6783–6820, 2015

CC BY

thetic energy flux. Both components are normally neglected due to their alleged small contribution (Foken, 2008a; Guo et al., 2009; Jacobs et al., 2008).

The uncertainty arising from the energy balance gap hampers the use of EC data for model parameterization and testing (Ingwersen et al., 2011; El Maayar et al., 2008; Falge et al., 2005). In these types of studies, in order to achieve an energy balance closure, the measured turbulent fluxes are usually adjusted with either the Bowen-ratio (BR), H flux or LE flux post-closure method. These methods fully add the residual to the measured turbulent fluxes, assuming that the available energy is measured correctly. The BR post-closure method assumes that the gap has the same Bowen ratio (Bo = H/LE) as the measured turbulent fluxes (Twine et al., 2000; Barr et al., 1994). In this case, adjusted LE flux (LE*, $\mathrm{W\,m^{-2}}$) is defined according to Eq. (3). The H post-closure method, letting the latent heat flux unaltered, adds the gap fully to the measured H flux (Ingwersen et al., 2011; Gayler et al., 2013). Oppositely, the LE flux post-closure method assigns the lacking energy fully to LE (Falge et al., 2005). There are also some model studies where the energy balance was left unclosed, so the raw, unadjusted energy fluxes were used (Staudt et al., 2010; Carrer et al., 2012).

$$\mathrm{LE}^* = \frac{R_\mathrm{n} - G}{Bo + 1} \tag{3}$$

The present study elucidates the nature of the energy balance gap over winter wheat in southwest Germany. For this purpose we (a) evaluated the energy balance of EC flux measurements over two vegetation seasons, additionally measuring evapotranspiration with the soil water balance method ($\mathrm{ET_{WB}}$), which does not depend on an a priori assumption on the composition of the energy residual, and (b) tested $\mathrm{ET_{EC}}$ adjusted by the BR, H or LE post-closure method against the $\mathrm{ET_{WB}}$.

2 Materials and methods

2.1 Study site

The present study was performed in Kraichgau (Fig. 1), one of the warmest regions in Germany. Mean annual temperature ranges between 9–10 °C, and precipitation between 730 and 830 mm per year. The rivers Neckar and Enz form the borders in the east. In the north and in the south, Kraichgau is bounded by the low mountain ranges of Odenwald and Black Forest. In the west, Kraichgau borders on the Upper Rhine plain. The Kraichgau area is about 1600 km^2 and a gently sloping hilly territory. Elevations vary between 200 and 320 m a.s.l. Soils, predominantly classified as Luvisols (IUSS Working Group WRB, 2007), were mostly formed here from periglacial loess, which accumulated during the last ice age. Today, the region is intensively used for agriculture. Around 53 % of the total area is used for crop production. Winter wheat, winter rape, summer barley, maize and sugar beet are the predominant crops.

The measurements were performed at the agricultural fields EC1 and EC3 belonging to the farm "Katharinentalerhof" (Fig. 1). The fields are located north of the city of Pforzheim (48.92° N, 8.70° E). The fields EC1 and EC3 are 14 and 15 ha large, respectively. The terrain is flat (elevation a.s.l.: 319 m). The predominant wind direction is south-west. Both fields are surrounded by agricultural fields, which are separated partly by tree-hedges. Two permanent pumping wells (installation depth 3 m) were used to monitor the groundwater table (see Fig. 1). The soil type at both fields is Stagnic Luvisol (IUSS Working Group WRB, 2007). Basic soil properties are given in Table 1. In both 2012 and 2013, fields were cropped with winter wheat (*Triticum aestivum* L. cv. Akteur). In both years, winter wheat was drilled on 17 October.

BGD
12, 6783–6820, 2015

2.2 Measurement of evapotranspiration

2.2.1 Eddy covariance technique

Using the EC technique, we measured the land surface exchange fluxes in a 30 min resolution. In 2012, the measurements were performed at EC3. In 2013, the measurements were repeated, but at EC1. Both sites were cropped with winter wheat. The EC method enables measuring the heat, energy and momentum exchange between land surface and atmosphere without disturbing the crop environment. Provided that the land surface is sufficiently flat and homogeneous, the exchange fluxes are one-dimensional and can be calculated from the covariance between vertical wind speed and the scalar of interest. In the case of the *LE* flux ($\mathrm{W\,m^{-2}}$) this leads to

$$\mathrm{LE} = \lambda\rho\overline{q'w'}, \tag{4}$$

where λ ($\mathrm{J\,kg^{-1}}$) and ρ ($\mathrm{kg\,m^{-3}}$) are the heat of vaporization and the density of air, respectively. The symbol q ($\mathrm{kg\,kg^{-1}}$) stands for the specific humidity of the air, and w ($\mathrm{m\,s^{-1}}$) denotes the vertical wind speed. The term $\overline{q'w'}$ is the covariance between the two quantities.

The EC stations were installed in the center of each study field in April 2009. The stations were equipped with an open path infrared CO_2/H_2O gas analyzer (Licor 7500, LI-COR Biosciences, USA) and a 3-D sonic anemometer (CSAT3, Campbell Scientific, UK). At EC3 (2012) the turbulent complex was installed at a height of 2.63 m. The Licor-CSAT3 separation distance was 0.22 m. The direction of Licor 7500 was 25° against north, CSAT3 orientation was 170°. At EC1 (2013), the turbulent complex was installed at a height of 3.10 m with a sensor separation of 0.12 m. Orientations of Licor 7500 and CSAT3 were 0 and 170°, respectively. Vertical wind speed and specific humidity were measured with 10 Hz frequency. All other sensors recorded data in 30 min intervals. Net radiation was measured with a NR01 4-component sensor (NR01, Hukseflux Thermal Sensors, the Netherlands). Air temperature and humidity were measured in 2 m height (HMP45C, Vaisala Inc., USA). Rainfall was measured using a tipping bucket

BGD
12, 6783–6820, 2015

(resolution: 0.2 mm per tip). The rain gauge (ARG100, Campbell Scientific Ltd., UK) was located close to the EC station. Soil sensors were also installed close to the EC station. Temperature probes (107 Thermistor probe, Campbell Scientific Inc., UK) were installed in 2, 6, 15, 30 and 45 cm depth. The volumetric water content was measured with TDR probes (CS616, Campbell Scientific Inc., UK) in 5, 15, 30, 45 and 75 cm depth. Three soil heat flux plates (HFP01, Huskeflux Thermal Sensors, the Netherlands) were installed in 8 cm depth. For measuring the hydraulic gradient at the lower boundary of the water balance domain, two matric potential sensors (257-L, Campbell Scientific Ink., UK) were installed in 130 cm and three sensors in 150 cm depth. The horizontal distance between sensors was about 50 cm.

The EC flux data were processed with the TK3.1 software (Mauder M., 2011). Surface energy fluxes were computed from 30 min covariances. Data points exceeding 4.5 SDs in a window of 15 values were labeled as spikes and were excluded from the time series. The planar fit coordinate rotation was applied to time periods of 10–14 days. Spectral losses were corrected according to Moore (1986). The fluctuation of sonic temperature was converted into actual temperature according to Schotanus et al. (1983). Density fluctuations were corrected by WPL (Webb et al., 1980). For data quality analysis we used the flag system after Foken (Mauder M., 2011). Half-hourly values with flags from 1 to 6 (high and moderate quality data) were used to calculate the energy balance closure and evapotranspiration. Gap filling of EC flux data was performed with the mean diurnal variation method using an averaging window of 14 days (Falge et al., 2001). Additionally we computed the random error of the fluxes, which consist of the instrumental noise error of the EC station and the stochastic (sampling) error (Mauder et al., 2013).

The EC ET (kg m^{-2} or mm) per half hour was estimated with the following equation:

$$\mathrm{ET_{EC}} = \frac{\mathrm{LE}}{\lambda} \times 1800\,\mathrm{s}, \quad (5)$$

BGD
12, 6783–6820, 2015

where the heat of vaporization as a function of temperature T (°C) (Foken, 2008b) was taken as

$$\lambda = 2\,501\,000 - 2370 \times T, \tag{6}$$

Subsequently, ET_{EC} values were adjusted by the H, LE or Bowen ratio post-closure method.

Ground heat flux was calculated as the sum of measured soil heat flux using the mean of the three soil heat flux plates and the heat storage change (ΔS_G) (Eq. 7) between the surface and the plates (Foken, 2008b)

$$\Delta S_G = \frac{C_v \times \Delta T \times L}{\Delta t}, \tag{7}$$

where C_v ($\mathrm{J\,m^{-3}\,°C^{-1}}$) is the volumetric heat capacity of the soil, ΔT (°C) denotes the soil temperature change during the period of time, Δt, considered, and L (m) is the thickness of the soil layer above the soil heat flux plates. The heat capacity of the soil was computed according to de Vries (1963) using the volumetric water content measured in 5 cm depth.

2.2.2 Soil water balance method

The water balance equation of a soil volume of a unit area and given depth reads as follows:

$$ET_{WB} = R - SP - SR - \Delta S \tag{8}$$

Here, R stands for rainfall, and SP is seepage (negative: capillary rise, positive: vertical drainage). The symbol SR denotes surface runoff and ΔS stands for the change in soil water storage over the balancing period. Based on our field observations, SR was negligible at the study sites during the periods considered.

BGD
12, 6783–6820, 2015

CC BY

ΔS was measured at sixteen positions. Sampling positions were distributed across the footprint of the EC station using a stratified random sampling design (Figs. 2b and 3b). The footprint area was determined with the forward Lagrangian stochastic footprint model described by Göckede et al. (2006) based on EC flux data measured in 2010 (EC3) and 2011 (EC1). In these years, the fields were also cropped with winter wheat (*Triticum aestivum* cv. Cubus (EC3) and cv. Akteur (EC1)). In the present study, we used the average footprint over stable, neutral and unstable atmospheric conditions. Footprint analyses were processed for periods from mid-May to late July, when the average plant height was about constant, on average 0.77 and 0.83 m at EC3 and EC1, respectively. The installation height of CSAT was 2.5 m at EC3 and 3.10 m at EC1 over the entire periods. The footprint model requires a land use and a roughness matrix as input files. Based on the satellite remote sensing data, we produced land use matrixes of the surroundings of the EC stations. The special spatial resolution of matrixes was 5 m and their areal coverage $500 \times 500\,m^2$. The subsequent land use types were counted: winter wheat, path, rape, grain, trees and suburban. Roughness values of the land use classes were taken from Foken (2008b) (Figs. 2a and 3a).

In 2012, we performed three soil sampling campaigns over the growing season: late April (25–27), mid-June (14–15) and late July (24–27). In 2013, four sampling campaigns were performed: mid-April (15–16), early June (3–4), mid-June (18–19) and late July (30–31). Soil samples were taken in 10 cm intervals down to 150 cm. For this purpose, three augers with a length of 60 cm (⌀ = 2.885 cm), 100 cm (⌀ = 2.386 cm) and 150 cm (⌀ = 1.763 cm) were used. The 60 cm auger was used for taking soil samples down to 60 cm. The 100 cm auger was used for sampling the 60–100 cm depth, and the 150 cm auger was taken for sampling between 100 to 150 cm. Soil samples were filled in plastic bags and transported to the lab within less than 10 h. Field wet soil samples were weighed, put into a ventilated oven and dried at 105 °C. Final weights were usually reached within 12 h. Based on mass balance, the gravimetric water content was calculated. It was converted to volumetric water content by multiplication with the bulk density. Bulk density of the topsoil layers (0–30 cm) was determined at each

BGD
12, 6783–6820, 2015

CC BY

sampling position using a cylindrical steel core cutter (diameter: 7.92 cm, volume for a 10 cm sampling depth: 492.7 cm^3) on 4 May in 2012 and on 30 April in 2013. In three 10 cm intervals the core cutter was inserted into the soil by careful turning. The soil sample was stored in a plastic bag and in the lab the soil dry weight was determined by drying the sample at 105 °C. Close to the EC station a pit was dug down to 150 cm. In the center of every 10 cm layer, 100 cm^3 of soil was sampled in triplicates using cylindrical cores ($\varnothing$ = 5.50 cm, height 4.21 cm). Bulk density was determined by drying the soil at 105 °C and determining its mass by weighing.

At the 140 cm depth we took soil samples to measure the water retention curve and the hydraulic conductivity function. Samples ($V = 250\,cm^3$, $\varnothing$ = 8 cm, 5 cm height) were taken in triplicates using sampling rings (UMS GmbH, Germany).

Additionally, soil texture was determined at each sampling position. Three layers (0–30, 30–60, 60–90, 90–120, and 120–150 cm) were pooled to one composite sample and soil texture was determined with the standard pipette method (Dane and Topp, 2002).

The seepage flux was computed from the Darcy–Buckingham law:

$$q_w = -K(h)\frac{\Delta H}{\Delta z} \tag{9}$$

Here, q_w ($cm\,d^{-1}$) is the water flux density, $K(h)$ ($cm\,d^{-1}$) denotes the hydraulic conductivity as a function of the matric potential h (cm), and H (cm) is the hydraulic potential, the sum of matric and gravitational potentials. The hydraulic gradient $\Delta H/\Delta z$ was computed from the matric potential measurements performed in 130 and 150 cm depth and the vertical separation distance Δz (cm) of the matric potential sensors.

The hydraulic conductivity function $K(h)$ was determined with the evaporation method according to Wind/Schindler using the HYPROP lab system (UMS GmbH, Germany). First, soil samples taken from the 140 cm depth were slowly saturated for 5–6 days. Afterwards soil samples were placed on a balance and exposed to evaporation. The matric potential was measured with micro-tensiometers in 1.25 and 3.75 cm depth.

CC BY

The soil sample weight and the matric potential were recorded automatically every minute at the first hour and every ten minutes in the next hours. After four to five days, the tensiometers fell dry and the measurement was stopped. The initial water content of soil samples was computed from their dry weight. Based on the acquired data, a water retention curve and hydraulic conductivity function were fitted to the data. Several hydraulic models (van Genuchten/Mualem (1980), bimodal van Genuchten/Mualem (Durner, 1994), Brooks and Corey (1964), Kosuqi (1996) and Fayer-Simmons, (1995) were tested. Parameters of the functions were fitted with the robust, non-linear optimizing procedure developed by Durner and Peters (2006) (*User Manual HYPROP*, 2012). The bimodal van Genuchten parameterization (Durner, 1994) was finally used to model $K(h)$ because it yielded the lowest Akaike information criterion (AICc):

$$K(h) = K_s \cdot \left[\sum_{j=1}^{2} w_j \left[1 + (a_j|h|)^{n_j} \right]^{1/n_j - 1} \right]^{\tau} \times \left[\frac{\sum_{j=1}^{2} w_j a_j \left\{ 1 - \left(a_j|h| \right)^{n_j - 1} \left[1 + (a_j|h|)^{n_j} \right]^{1/n_j - 1} \right\}}{\sum_{j=1}^{2} w_j a_j} \right]^2 \quad j = (1,2) \tag{10}$$

In Eq. (10), K_s ($\mathrm{cm\,d^{-1}}$) is saturated hydraulic conductivity, w_j are the weighting factors of two van Genuchten functions and a_j, n_j are the shape parameters of the two retention curves. The tortuosity factor τ was set to 0.5. K_S was measured on soil samples taken at EC1 from 140 cm depth by the falling head technique using a KSAT system (UMS GmbH, Germany). The methodology of the device follows the German standard DIN 18130-1 and is based on the inversion of the Darcy law (Operation Manual KSAT, 2013). Measurement of K_S was repeated five times with each of three samples. The average value of K_S was 39.3 $\mathrm{cm\,day^{-1}}$.

BGD
12, 6783–6820, 2015

Energy balance closure on a winter wheat stand

K. Imukova et al.

CC BY

In 2013, we additionally measured the volumetric soil water content with capacitance soil moisture probes (SM1, Adcon Telemetry, Austria). The probes were installed on 17 and 18 December 2012. The soil moisture network consisted of sixteen stations located at the same positions where soil samples were taken (Fig. 3b). Every station was situated in the middle between two machine tracks, so the farmer could easily pass the station during fertilization and pesticide application. Each station consisted of a nine-level SM1 capacitance probe, remote transfer unit (RTU) (addIT A723 Series 4, Adcon Telemetry, Austria) and a solar panel for power supply.

Adcon SM1 sensors measure the capacitance and are characterized by low power consumption. Their radius of influence is about 10 cm. In order to install the SM1 probes, we removed the soil with a screw auger and then carefully installed the moisture sensors. To avoid air voids between sensor and soil, the bore hole was carefully filled up with soil slurry. The RTU and solar panel were mounted to an aluminum mast and installed about 2 m away from the SM1 sensor.

The volumetric water content was measured for 15 min intervals at 10 cm resolution down to 90 cm depth. Soil moisture content was measured from 1 April to 4 August 2013. Each RTU stored and transmitted the data to the so-called master station (RA440, Adcon Telemetry, Austria) mounted on the EC mast. The master station transferred the data via GSM modem to the central data server (A850 Telemetry Gateway, Adcon Telemetry GmbH, Austria) located at the University of Hohenheim.

The SM1 sensors were calibrated separately using the data of the four sampling campaigns in 2013 described above. Soil samples were taken about 30–50 cm away from the sensor. The calibration line was derived by regressing θ_v measured by the sensor to θ_v measured in the lab.

Mean diurnal ET_{WB} and ET_{EC}, adjusted by the BR, H or LE post-closure methods, were estimated and compared in 6 OPs (OP) (Tables 2 and 3). In OP-1, OP-2, OP-3 and OP-6, ET_{WB} was estimated based on data obtained during the soil sample campaigns, whereas in OP-4 and OP-5 it was estimated based on the data of SM1 sensors.

BGD
12, 6783–6820, 2015
Energy balance closure on a winter wheat stand
K. Imukova et al.

CC BY

The last two periods are characterized by low precipitation and seepage, which helps minimize uncertainties in drainage calculations (Fig. 8).

2.3 Error estimation

The error of measured ET_{WB} was estimated assuming the Gaussian error propagation law (Currell et al., 2009):

$$s_y = \sqrt{\left(\frac{\partial y}{\partial x}\right)^2 s_x^2 + \left(\frac{\partial y}{\partial k}\right)^2 s_k^2 + \left(\frac{\partial y}{\partial z}\right)^2 s_z^2 + \ldots} \quad (11)$$

Here, s_y is the SD of the function y with measurements *x, k, z* and so forth [$y = f(x, k, z\ldots)$]; s_x, s_k and s_z are the SDs of the x, k and z measurements, respectively; $\partial y/\partial x$ is the partial derivative of the function y with respect to x, etc.

The standard errors (SE) of R, SP and ΔS were estimated from the SD of the measurement s and the number of observations, n:

$$\mathrm{SE} = \frac{s}{\sqrt{n}} \quad (12)$$

3 Results

3.1 Energy balance closure of eddy covariance data

The EBC of high-quality data (1–3 flags after Foken) and excluding low LE fluxes ($-25\,\mathrm{W\,m^{-2}} < \mathrm{LE} < 25\,\mathrm{W\,m^{-2}}$) was 73 % during the vegetation period 2012 and 67 % from mid-June to late July in 2013. The average random error was 16 % for both LE and H in 2012. In 2013, the random error of LE was 12 % and that of H was 14 %. In total, 43 % of the data fulfilled the above quality criteria. Allowing in addition for moderate quality data (4–6 flags after Foken), EBC decreased on average by about 2 and

4 % in 2012 and 2013, respectively. Table 3 summarizes the EBC in different OPs estimated based on high and moderate quality data. In 2012, from late April to late July the average EBC was about 71 %. This EBC was uniform during different OPs. The average residual was 68.5 $W m^{-2}$. The random error of LE was 18 %, that of H 19 %. In 2013, we observed a lower EBC of about 60 %. The average residual was 86.1 $W m^{-2}$. The average random error of flux measurements was 16.5 % for LE and 18 % for H. The lowest EBC of about 57 % was measured from mid-April to early June. During this period, 55 % of days were rainy days (Fig. 8) resulting in a large amount of rainfall (250 mm) – about 50 % higher than in 2012 (Table 2). In this period we also measured the lowest net radiation and vapor pressure deficit (data not shown). At the end of the vegetation period, EBC increased. Figure 5 shows the diurnal cycles of the energy fluxes as well as energy residual during the different OPs. Figure 4 shows graphically EBC in both years. The slope of the regression line, forced through the origin, of the available energy on the turbulent energy was 0.71 in 2012. In 2013 it was 0.64.

3.2 Evapotranspiration measurements

3.2.1 Vegetation period 2012

The two pumping wells stayed dry over the whole vegetation period (OP-1), i.e., the groundwater level was always deeper than three meters. Total rainfall was 275 mm and seepage amounted to 13 mm (Table 3). During the first soil sample campaign, 486.3 mm of water were stored in the upper 150 cm of soil (Fig. 6). The soil water stock decreased by 44.6 to 441.7 mm. During OP-2, soil water storage was depleted to 426.3 mm. During OP-3, rainfall refilled the soil water stock by 15.4 mm. The vertical soil water profiles showed the largest differences within the upper 100 cm of the soil profile. Below 100 cm the soil water content changed only very little (Fig. 6). The components of the soil water balance and the resulting ET are compiled and compared with ET_{EC} in Table 3. In all OPs, the best agreement of the EC technique with WB method was achieved without adjusting the LE flux data (H post-closure method). The ET_{EC}

BGD
12, 6783–6820, 2015

computed with the Bowen ratio method was on average about 21 % higher than ET_{WB}. The ET_{EC} computed with the LE flux post-closure method was on average about 34 % higher than ET_{WB}.

3.2.2 Vegetation period 2013

Between mid-April and early June 2013, rainfall was more than twice as high as in 2012 (data not shown). The water level in the pumping wells rose to the surface for several days during this period (8 May and 3–5 June), and surface runoff was observed at the field. In this period, temperatures and vapor pressure deficits were low (data not shown). During this period, marked on Fig. 7 as OP-0, the soil water stock was filled up by 57.9 mm. Due to exceptionally high rainfall and surface runoff, the calculation of the terms SP and SR of the water balance equation is unreliable, which hampered comparing the EC and WB methods.

In OP-6, soil water storage decreased by 105.2 to 398.7 mm (Fig. 7). The total rainfall for this period was about 50 % less than that in 2012 (Table 2). Seepage was low, about 3 mm, over this period. Table 3 compares ET_{WB} with ET_{EC}. In OP-6, better agreement of the EC technique with WB method was achieved by adjusting the LE flux data with the BR and *H* post-closure method. The ET_{EC} post-closed with the BR method was about 15 % higher than the ET_{WB}. The ET_{EC} computed with the *H* post-closure method was about 18 % lower than the ET derived from the WB method. The ET_{EC} adjusted with the LE post-closure method was 26 % higher than the ET_{WB}.

Soil water profiles of OP-4 and OP-5 are shown in Fig. 7. ET_{WB} agreed best with non-adjusted raw ET_{EC} (H post-closure method), while BR and LE post-closure methods significantly overestimated ET by about 30 and 40 %, respectively (Table 3).

BGD
12, 6783–6820, 2015

CC BY

4 Discussion

The EBCs of the present study agree with those of other studies performed over agricultural land, where EBCs are typically characterized by high energy residuals (20–40 %) (Charuchittipan et al., 2014; Foken, 2008a; Panin et al., 2008; Stoy et al., 2013). The random errors of our EC fluxes are also in a good agreement with random errors reported by Mauder (2013) and Foken (2008a). They are typically between 5 and 20 % for high-quality data.

The differences between EC1 and EC3 with regard to EBC might be partly assigned to the heterogeneity of the surroundings (Stoy et al., 2013). The field of view of the flux sensor depends, among others, on the wind direction, surrounding land uses and measurement height. In the case of EC 3, predominant south-west winds cross the study area without any obstacles, forming a relatively compact ellipse-shape footprint (Fig. 2). The source area of EC1 was larger than that of EC3 and widened mainly to the south-west, where a hilly forested area is situated about 500 m away from the station (Figs. 3 and 1). Here, large eddies may have been formed at the boundary between the two land covers (Foken, 2008b). Large eddies are non-uniformly distributed. They do not touch the land surface and cannot be detected by EC stations. Several authors (Klaassen et al., 2006; Friedrich et al., 2000) reported an increase of the turbulent fluxes at forest edges. Energy transfer by large eddies has to be modeled or measured with an area-averaging method (Foken, 2008a; Stoy et al., 2013). Kanda (2004) and Inagaki (2006) used large eddy simulations (LES) to study the contribution of large eddies to energy exchange. They concluded that the spatially averaged fluxes were able to resolve the closure problem. As mentioned already in the Introduction, however, this large eddy theory has not been fully embraced by the scientific community (see e.g., Leuning et al., 2012).

Our experiment also showed the limits of the WB method imposed by the prevailing weather conditions. It was not possible to reliably estimate ET_{WB} in periods with heavy rain due to the uncertainties in drainage calculation and surface runoff. Ideal conditions

CC BY

for performing the WB method are periods with low precipitation and low or absent seepage, and with soil water contents below field capacity (Schume et al., 2005; Wilson et al., 2001).

The comparison of the two methods shows that the EC method reliably measures evapotranspiration when no adjustment is applied (Fig. 9). Similar results were obtained in other experimental studies. Schume (2005) cross-checked ET measured with the EC technique against the soil water balance method over a mixed European beech–Norway spruce forest. The observed EBC ranged between 73 to 92 % at their study site. They demonstrated that ET was adequately measured with the EC technique. They concluded that the proportional distribution of the residual between the energy balance components would lead to an overestimation of LE. Wilson (2001) compared non-adjusted ET_{EC} with ET measured by various other measurement techniques. EBC was 80 %. They reported a good agreement between ET_{EC} and ET assessed by the catchment water balance method. Both methods estimated nearly equal annual ET over a 5 year period. They also observed a high correlation between ET_{EC} and ET assessed by the soil water budget method. Nonetheless, the data were highly variable during periods with rainfall and rapid water movement within the soil profile.

There are some more studies, which point to the fact that the EC technique reliably measured LE without applying any post-closure method. Wolf and Laca (2007) performed a cospectra analysis of the ET_{EC} measured over short-grass steppes. They found that H flux was underestimated by 14 % due to the lack of measurement resolution in the high-frequency range. The LE loss was only half of the H loss. He concluded that this must lead to a bias in the measured Bowen ratio. Mauder (2006) estimated the low-frequency loss of EC flux data. He reported that the commonly used 30 min averaged interval of the covariances does not cover the entire spectrum of the turbulent fluxes. Extending the average time substantially reduced the residual, considerably increasing H flux yet leaving LE practically unaltered. H changed from 40.1 $W\,m^{-2}$ with a 5 min averaging interval to 66.9 $W\,m^{-2}$ with 24 h. LE, in contrast, decreased from

BGD
12, 6783–6820, 2015
Energy balance closure on a winter wheat stand
K. Imukova et al.

CC BY

$73.9\,\mathrm{W\,m^{-2}}$ with 5 min averaging interval to $66.9\,\mathrm{W\,m^{-2}}$ with 24 h, although with an averaging time of multiple days, LE was about $75\,\mathrm{W\,m^{-2}}$.

Contrasting results were obtained in other similar studies, i.e. where independently measured ET was compared with ET_{EC}. For instance, Barr (2012) compared measured streamflow from the watershed with streamflow, estimated from seven flux towers in this watershed, over a 10 year period. The annual EBC was about 85 % across sites and years. His results showed that measured streamflow better agreed with outflow estimated based on the ET_{EC} adjusted with the BR method, whereas outflow based on the raw ET_{EC} flux was about 40 % higher. In several other experimental studies, independently measured ET agreed better with ET_{EC} adjusted by one of the post-closure methods. Wohlfahrt (2010) cross-checked ET_{EC} against ET determined using micro-lysimeters and an approach scaling up leaf-level stomatal conductance to canopy-level transpiration. The observed EBC was about 85 %. The best correspondence between EC and the independent methods was achieved with the LE post-closure method. Cuenca (1997) conducted intensive field campaigns (IFC) in spring and summer using a neutron probe and time domain reflectometry to evaluate the soil water content at a boreal forest. During IFC-1 he reported a good agreement between unadjusted ET_{EC} ($2.9\,\mathrm{mm\,day^{-1}}$) and ET estimated based on the soil water profile analysis ($2.6\,\mathrm{mm\,day^{-1}}$). During IFC-2, however, the difference between the two methods was extremely high: $3.6\,\mathrm{mm\,day^{-1}}$ against $2.1\,\mathrm{mm\,day^{-1}}$, respectively. They related this difference to the spatial differences and sampling volume of the measurement techniques. They also suggested that the ET_{WB} vs. ET_{EC} difference could be due to the underestimation by the turbulent complex of the downward (negative) LE flux at night, which would overestimate the LE flux.

Our results synthesized with the findings from literature suggest that there is no universal approach to post-close the energy balance gap. The composition of the energy residual seems to be site-specific. Therefore, it is advisable to perform for each site an independent measurement of LE to identify the most suitable post-closure method.

cc BY

Our results imply that, at our study site during most periods of the season, the energy balance gap is not made up by latent heat. Other fluxes or storage terms must account for closing the energy balance gap. Possible candidates are underestimated sensible heat and/or ground heat fluxes. Moreover, vertical advection due to non-zero vertical wind speed (Foken, 2008a; Oncley et al., 2007) or the loss of low- and/or high-frequency components may partly explain the gap. The energy balance gap might also be caused by neglected terms such as energy storage in the canopy and energy consumption during photosynthesis. Although it is commonly assumed that the energy consumption by photosynthesis is negligible, Meyers (2004) demonstrated that photosynthetic energy flux can reach, on a half-hourly basis, up to 30 $W m^{-2}$ at midday. He observed a maximum of the canopy heat storage in the early morning hours (up to 20 $W m^{-2}$). Combining soil heat storage with canopy heat and photosynthetic energy flux improved the EBC by 15 and 7 % for fully developed maize and soybean field, respectively. Oncley (2007) observed that the average heat storage by the canopy was about 10 $W m^{-2}$ on a flood-irrigated cotton field, whereas the photosynthetic energy flux peaked at 48 $W m^{-2}$ with a diurnal average of 8 $W m^{-2}$. Jacobs (2008) showed that EBC could be improved by 6 % at a grassland by considering energy consumption by photosynthesis and other minor storage terms such as enthalpy storage in the air layer between turbulent complex and the land surface. Lamaud (2001) achieved a nearly perfect EBC in the understory of a forest canopy by considering the heat storage within and by the canopy as well as photosynthesis. Guo (2009) observed a decrease of EBC with the physiological development of maize. EBC was about 89 % on bare soil and 67 % during the senescence phase of the maize at the same field. Accordingly, the study concluded that heat storage and photosynthesis energy of the vegetation canopy play an important role in energy balance closure.

5 Conclusions

We cross-checked the latent heat flux data obtained with the EC method against LE fluxes measured with the soil water balance method. Both measurements were performed at winter wheat stands in two years, 2012 and 2013. At the study site, both the Bowen-ratio and the LE post-closure method led to substantially higher ET than the WB method. In general, ET measured with the WB method agreed best with the raw non-adjusted ET fluxes (H post-closure method). Only at the end of 2013 vegetation season, during a period with high and frequent rainfall, ET_{WB} was in-between the ET_{EC} adjusted by the *H* and Bowen ratio method, respectively. Our study also illustrates the limits of the WB method. The lower the rainfall and seepage, the more reliable the measurement. At our study site, the energy balance gap during most periods of the season was not made up by latent heat. This calls for considering other fluxes or storage terms to even out the energy balance.

Acknowledgements. The present study was supported by the German Research Foundation (DFG) in the framework of the Research Unit (RU) 1695 "Structure and function of agricultural landscapes under global climate change – Processes and projections on regional scale" and in part by Erasmus Mundus grant SGA 2010-2361. We thank Benedikt Prechter and Maxim Poltoradnev for the great help in conducting the soil sampling campaigns and installing the soil moisture network.

References

Barr, A. G., King, K. M., Gillespie, T. J., den Hartog, G., and Neumann, H. H.: A comparison of Bowen ratio and eddy correlation sensible and latent heat flux measurements above deciduous forest, Bound.-Layer Meteorol., 71, 21–41, 1994.

Barr, A. G., van der Kamp, G., Black, T. A., McCaughey, J. H., and Nesic, Z.: Energy balance closure at the BERMS flux towers in relation to the water balance of the White Gull Creek watershed 1999-2009, Agr. Forest Meteorol., 153, 3–13, 2012.

BGD
12, 6783–6820, 2015

CC BY

Brooks, R. H. and Corey, A. T.: Hydraulic properties of porous media, Colorado State Univ., Fort Collins, Hydrol. Pap., 3, 1–27, 1964.

Carrer, D., Lafont, S., Roujean, J., Calvet, J., Meurey, C., Le Moigne, P., and Trigo, I. F.: Incoming solar and infrared radiation derived from METEOSAT: impact on the modeled land water and energy budget over France, J. Hydrometeorol., 13, 504–520, 2012.

Charuchittipan, D., Babel, W., Mauder, M., Leps, J., and Foken, T.: Extension of the averaging time in eddy-covariance measurements and its effect on the energy balance closure, Bound.-Layer Meteorol., 152, 303–327, 2014.

Cuenca, R. H., Stangel, D. E., and Kelly, S. F.: Soil water balance in a boreal forest, J. Geophys. Res.-Atmos., 102, 29355–29365, 1997.

Currell, G. and Dowman, A.: Essential mathematics and statistics for science, The University of the West of England, UK, 2009.

Dane, J. H. and Topp, G. C.: Methods of soil analysis, Part 4 – Physical methods: Soil Science Society of America Book Series No. 5, Soil Science Society of America, Madison, Wisconsin, 2002.

Durner, W.: Hydraulic conductivity estimation for soils with heterogeneous pore structure, Water Resourc. Res., 30, 211–223, 1994.

El Maayar, M., Chen, J. M., and Price, D. T.: On the use of field measurements of energy fluxes to evaluate land surface models, Ecol. Model., 214, 293–304, 2008.

Falge, E., Baldocchi, D., Olson, R., Anthoni, P., Aubinet, M., Bernhofer, C., Burba, G., Ceulemans, R., Clement, R., Dolman, H., Granier, A., Gross, P., Grünwald, T., Hollinger, D., Jensen, N. -., Katul, G., Keronen, P., Kowalski, A., Lai, C. T., Law, B. E., Meyers, T., Moncrieff, J., Moors, E., Munger, J. W., Pilegaard, K., Rannik, Ü, Rebmann, C., Suyker, A., Tenhunen, J., Tu, K., Verma, S., Vesala, T., Wilson, K., and Wofsy, S.: Gap filling strategies for defensible annual sums of net ecosystem exchange, Agr. Forest Meteorol., 107, 43–69, 2001.

Falge, E., Reth, S., Brüggemann, N., Butterbach-Bahl, K., Goldberg, V., Oltchev, A., Schaaf, S., Spindler, G., Stiller, B., Queck, R., Köstner, B., and Bernhofer, C.: Comparison of surface energy exchange models with eddy flux data in forest and grassland ecosystems of Germany, Ecol. Model., 188, 174–216, 2005.

Fayer, M. J. and Simmons, C. S.: Modified soil water retention functions for all matric suctions, Water Resour. Res., 31, 1233–1238, 1995.

CC BY

Foken, T.: The energy balance closure problem: an overview, Ecol. Appl., 18, 1351–1367, 2008a.
Foken, T.: Micrometeorology, Micrometeorology, Springer, Heidelberg, 308 pp., 2008b.
Foken, T. and Wichura, B.: Tools for quality assessment of surface-based flux measurements, Agr. Forest Meteorol., 78, 83–105, 1996.
Foken, T., Mauder, M., Liebethal, C., Wimmer, F., Beyrich, F., Leps, J., Raasch, S., DeBruin, H. A. R., Meijninger, W. M. L., and Bange, J.: Energy balance closure for the LITFASS-2003 experiment, Theor. Appl. Climatol., 101, 149–160, 2010.
Friedrich, K., Mölders, N., and Tetzlaff, G.: On the influence of surface heterogeneity on the Bowen-Ratio: a theoretical case study, Theor. Appl. Climatol., 65, 181–196, 2000.
Gayler, S., Ingwersen, J., Priesack, E., Wöhling, T., Wulfmeyer, V., and Streck, T.: Assessing the relevance of subsurface processes for the simulation of evapotranspiration and soil moisture dynamics with CLM3.5: comparison with field data and crop model simulations, Environ. Earth Sci., 69, 415–427, 2013.
Göckede, M., Markkanen, T., Hasager, C. B., and Foken, T.: Update of a footprint-based approach for the characterisation of complex measurement sites, Bound.-Layer Meteorol., 118, 635–655, 2006.
Guo, J. X., Bian, L. G., and Dai, Y. J.: Multiple time scale evaluation of the energy balance during the maize growing season, and a new reason for energy imbalance, Sci. China Ser. D, 52, 108–117, 2009.
Heusinkveld, B. G., Jacobs, A. F. G., Holtslag, A. A. M., and Berkowicz, S. M.: Surface energy balance closure in an arid region: role of soil heat flux, Agr. Forest Meteorol., 122, 21–37, 2004.
Inagaki, A., Letzel, M. O., Raasch, S., and Kanda, M.: Impact of surface heterogeneity on energy imbalance: A study using LES, J. Meteorol. Soc. Jpn., 84, 187–198, 2006.
Ingwersen, J., Steffens, K., Högy, P., Warrach-Sagi, K., Zhunusbayeva, D., Poltoradnev, M., Gäbler, R., Wizemann, H., Fangmeier, A., Wulfmeyer, V., and Streck, T.: Comparison of Noah simulations with eddy covariance and soil water measurements at a winter wheat stand, Agr. Forest Meteorol., 151, 345–355, 2011.
IUSS Working Group WRB: World Reference Base for Soil Resources 2006, First Update 2007, World Soil Resources Reports, FAO, Rome, 2007.
Jacobs, A. F. G., Heusinkveld, B. G., and Holtslag, A. A. M.: Towards closing the surface energy budget of a mid-latitude grassland, Bound.-Layer Meteorol., 126, 125–136, 2008.

Kanda, M., Inagaki, A., Letzel, M. O., Raasch, S., and Watanabe, T.: Les study of the energy imbalance problem with eddy covariance fluxes, Bound.-Layer Meteorol., 110, 381–404, 2004.
Klaassen, W. and Sogachev, A.: Flux footprint simulation downwind of a forest edge, Bound.-Layer Meteorol., 121, 459–473, 2006.
Kosugi, K.: Lognormal distribution model for unsaturated soil hydraulic properties, Water Resour. Res., 32, 2697–2703, 1996.
Lamaud, E., Ogée, J., Brunet, Y., and Berbigier, P.: Validation of eddy flux measurements above the understorey of a pine forest, Agr. Forest Meterol., 106, 187–203, 2001.
Leuning, R., van Gorsel, E., Massman, W. J., and Isaac, P. R.: Reflections on the surface energy imbalance problem, Agric. For. Meterol., 156, 65–74, 2012.
Mauder, M. and Foken, T.: Impact of post-field data processing on eddy covariance flux estimates and energy balance closure, Meteorol. Z., 15, 597–609, 2006.
Mauder, M. and Foken, T.: Documentation and Instruction Manual of the Eddy-Covariance Software Package TK3. Arbeitsergebnisse Nr. 46, Universität Bayreuth, Abteilung Mikrometeorologie, ISSN 1614-8916, Bayreuth, 2011.
Mauder, M., Desjardins, R. L., and MacPherson, I.: Scale analysis of airborne flux measurements over heterogeneous terrain in a boreal ecosystem, J. Geophys. Res.-Atmos., 112, D13112, doi:10.1029/2006JD008133, 2007.
Mauder, M., Cuntz, M., Drüe, C., Graf, A., Rebmann, C., Schmid, H. P., Schmidt, M., and Steinbrecher, R.: A strategy for quality and uncertainty assessment of long-term eddy-covariance measurements, Agr. Forest Meteorol., 169, 122–135, 2013.
Meyers, T. P. and Hollinger, S. E.: An assessment of storage terms in the surface energy balance of maize and soybean, Agr. Forest Meteorol., 125, 105–115, 2004.
Moore, C. J.: Frequency response corrections for eddy correlation systems, Bound.-Layer Meteorol., 37, 17–35, 1986.
Oncley, S. P., Foken, T., Vogt, R., Kohsiek, W., DeBruin, H. A. R., Bernhofer, C., Christen, A., van Gorsel, E., Grantz, D., Feigenwinter, C., Lehner, I., Liebethal, C., Liu, H., Mauder, M., Pitacco, A., Ribeiro, L., and Weidinger, T.: The energy balance experiment EBEX-2000. Part I: Overview and energy balance, Bound.-Layer Meteorol., 123, 1–28, 2007.
Panin, G. N. and Bernhofer, C.: Parametrization of turbulent fluxes over inhomogeneous landscapes, Izv. Atmos. Ocean Phys., 44, 701–716, 2008.
Sakai, R. K., Fitzjarrald, D. R., and Moore, K. E.: Importance of low-frequency contributions to eddy fluxes observed over rough surfaces, J. Appl. Meteorol., 40, 2178–2192, 2001.

Schotanus, P., Nieuwstadt, F. T. M., and De Bruin, H. A. R.: Temperature measurement with a sonic anemometer and its application to heat and moisture fluxes, Bound.-Layer Meteorol., 26, 81–93, 1983.

Schume, H., Hager, H., and Jost, G.: Water and energy exchange above a mixed European Beech - Norway Spruce forest canopy: A comparison of eddy covariance against soil water depletion measurement, Theor. Appl. Climatol., 81, 87–100, 2005.

Staudt, K., Falge, E., Pyles, R. D., Paw U, K. T., and Foken, T.: Sensitivity and predictive uncertainty of the ACASA model at a spruce forest site, Biogeosciences, 7, 3685–3705, doi:10.5194/bg-7-3685-2010, 2010.

Stoy, P. C., Mauder, M., Foken, T., Marcolla, B., Boegh, E., Ibrom, A., Arain, M. A., Arneth, A., Aurela, M., Bernhofer, C., Cescatti, A., Dellwik, E., Duce, P., Gianelle, D., van Gorsel, E., Kiely, G., Knohl, A., Margolis, H., Mccaughey, H., Merbold, L., Montagnani, L., Papale, D., Reichstein, M., Saunders, M., Serrano-Ortiz, P., Sottocornola, M., Spano, D., Vaccari, F., and Varlagin, A.: A data-driven analysis of energy balance closure across FLUXNET research sites: the role of landscape scale heterogeneity, Agr. Forest Meteorol., 171–172, 137–152, 2013.

Tsvang, L. R., Fedorov, M. M., Kader, B. A., Zubkovskii, S. L., Foken, T., Richter, S. H., and Zeleny, Y.: Turbulent exchange over a surface with chessboard-type inhomogeneities, Bound.-Layer Meteorol., 55, 141–160, 1991.

Twine, T. E., Kustas, W. P., Norman, J. M., Cook, D. R., Houser, P. R., Meyers, T. P., Prueger, J. H., Starks, P. J., and Wesely, M. L.: Correcting eddy-covariance flux underestimates over a grassland, Agr. Forest Meteorol., 103, 279–300, 2000.

UMS GmbH: Operation Manual KSAT, Germany, 2013.

UMS GmbH: User Manual HYPROP, Germany, 2012.

Webb, E. K., Pearman, G. I., and Leuning, R.: Correction of flux measurements for density effects due to heat and water vapour transfer, Q. J. Roy. Meteor. Soc., 106, 85–100, 1980.

Wilson, K., Goldstein, A., Falge, E., Aubinet, M., Baldocchi, D., Berbigier, P., Bernhofer, C., Ceulemans, R., Dolman, H., Field, C., Grelle, A., Ibrom, A., Law, B. E., Kowalski, A., Meyers, T., Moncrieff, J., Monson, R., Oechel, W., Tenhunen, J., Valentini, R., and Verma, S.: Energy balance closure at FLUXNET sites, Agr. Forest Meteorol., 113, 223–243, 2002.

Wilson, K. B., Hanson, P. J., Mulholland, P. J., Baldocchi, D. D., and Wullschleger, S. D.: A comparison of methods for determining forest evapotranspiration and its components: Sap-flow,

soil water budget, eddy covariance and catchment water balance, Agr. Forest Meteorol., 106, 153–168, 2001.
Wohlfahrt, G., Irschick, C., Thalinger, B., Hörtnagl, L., Obojes, N., and Hammerle, A.: Insights from independent evapotranspiration estimates for closing the energy balance: a grassland case study, Vadose Zone J., 9, 1025–1033, 2010.
Wolf, A. and Laca, E. A.: Cospectral analysis of high frequency signal loss in eddy covariance measurements, Atmos. Chem. Phys. Discuss., 7, 13151–13173, doi:10.5194/acpd-7-13151-2007, 2007.

BGD
12, 6783–6820, 2015

CC BY

Table 1. Basic soil properties of the fields EC1 and EC3. At both sites the soil type is Stagnic Luvisol (IUSS Working Group WRB, 2007).

Depth (cm)	Bulk density ($g\,cm^{-3}$)	Texture S/U/C* (% by weight)	Organic matter content (% by weight)	Carbonate content (% by weight)	pH (0.01 M $CaCl_2$)
EC1					
0–30	1.49	3.4/81.2/15.4	1.54	0.21	6.9
30–60	1.50	3.4/81.6/15.0	0.31	0.29	6.7
60–90	1.47	2.8/81.6/15.6	0.27	0.31	6.6
90–120	1.47	2.8/81.1/16.1	0.53	0.27	6.6
120–150	1.48	2.4/80.0/17.6	0.33	0.37	6.6
EC3					
0–30	1.43	3.4/81.2/15.4	1.60	0.13	6.4
30–60	1.49	3.7/80.6/15.7	0.31	0.10	6.5
60–90	1.47	2.3/80.9/16.7	0.62	0.12	6.6
90–120	1.51	1.8/80.5/17.7	0.40	0.13	6.6
120–150	1.55	1.5/80.3/18.2	0.34	0.05	6.6

* Fraction of sand (S), silt (U), clay (C).

BGD
12, 6783–6820, 2015

CC BY

Table 2. Weather conditions in the observation periods (OPs) 2012 and 2013.

Vegetation period, year	2012			2013		
Observation period (OP)	25 Apr–27 Jul OP-1	25 Apr–15 Jun OP-2	14 Jun–27 Jul OP-3	13 Apr–26 Apr OP-4	05 Jul–27 Jul OP-5	18 Jun–31 Jul OP-6
Mean net radiation, $W m^{-2}$	148.9	146.9	152.6	119.1	192.7	173.3
Mean temperature, °C	16.1	14.6	17.9	12.8	19.9	18.6
Mean wind speed, $m s^{-1}$	1.6	1.7	1.5	2.3	1.4	1.6
Vapor pressure deficit, hPa	6.4	5.9	6.9	6.1	10.2	8.2
Bowen ratio (H/LE)	0.8	0.6	1.0	0.4	1.1	1.0
Rainfall, mm	275	124	151	6	1.4	67

BGD
12, 6783–6820, 2015

Energy balance closure on a winter wheat stand

K. Imukova et al.

Table 3. Evapotranspiration measured with the water balance (WB) method and the eddy co-variance (EC) technique at winter wheat stands in 2012 and 2013.

Vegetation period, year	2012			2013		
Observation period (OP)	25 Apr–27 Jul OP-1	25 Apr–15 Jun OP-2	14 Jun–27 Jul OP-3	13 Apr–26 Apr OP-4	5 Jul–27 Jul OP-5	18 Jun–31 Jul OP-6
Length of the period, days	94	52	44	14	23	44
Rainfall, mm	275	124	151	6	1.4	67
Water storage, mm	−44.6	−60	15.4	−24.5	−67.9	−105.2
Drainage/capillary rise, mm	16.8/3.9	9.9/2.1	7.2/1.9	0.2/2.9	0.2/2.6	1.4/4.2
Average evapotranspiration, mm day^{-1}						
WB method	3.3 ± 0.3	3.4 ± 0.3	3.0 ± 0.4	2.4 ± 0.5	3.1 ± 0.3	3.9 ± 0.4
EC method with sensible heat flux post-closure method	3.4 ± 0.6	3.5 ± 0.6	3.3 ± 0.6	2.3 ± 0.4	3.1 ± 0.5	3.2 ± 0.5
EC method with Bowen ratio post-closure method	4.1 ± 0.6	4.3 ± 0.7	3.9 ± 0.6	3.3 ± 0.5	4.6 ± 0.7	4.5 ± 0.7
EC method with latent heat flux post-closure method	4.9 ± 0.9	5.1 ± 1.0	4.8 ± 0.8	3.8 ± 0.7	5.4 ± 0.9	5.3 ± 0.9
Energy balance closure (EBC)						
Average EBC, %	71	70	72	55	62	63
Average residual, W m^{-2}	68.5	72.4	65.1	70.6	98.8	89.1
Number of data	2542 (57.0 %)	1426 (57.7 %)	1170 (56.1 %)	391 (58.2 %)	695 (63.0 %)	1269 (60.7 %)

BGD
12, 6783–6820, 2015
Energy balance closure on a winter wheat stand
K. Imukova et al.

CC BY

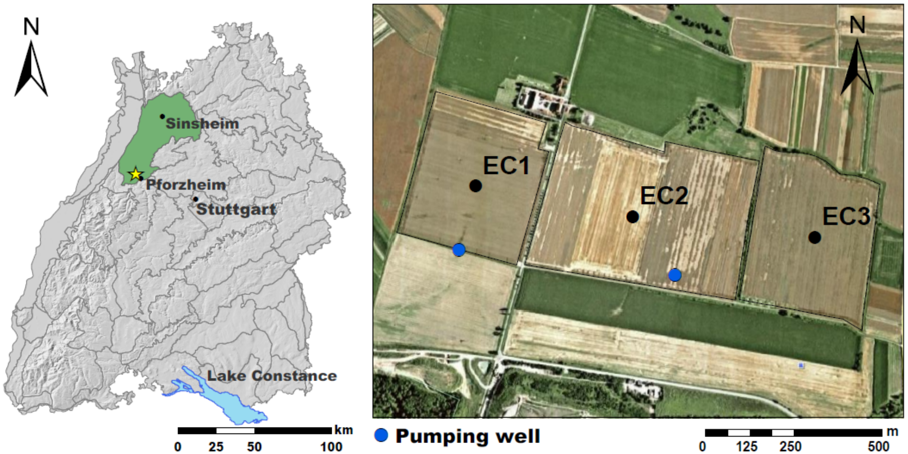

Figure 1. The study region "Kraichgau" (green) on the map of the federal state Baden-Württemberg. Location of the central study site is indicated by a yellow star. The right panel shows a close-up of the central study site. That site consists of three fields (EC1-3). An eddy covariance station (black full point) is installed in the center of each field.

BGD
12, 6783–6820, 2015

cc BY

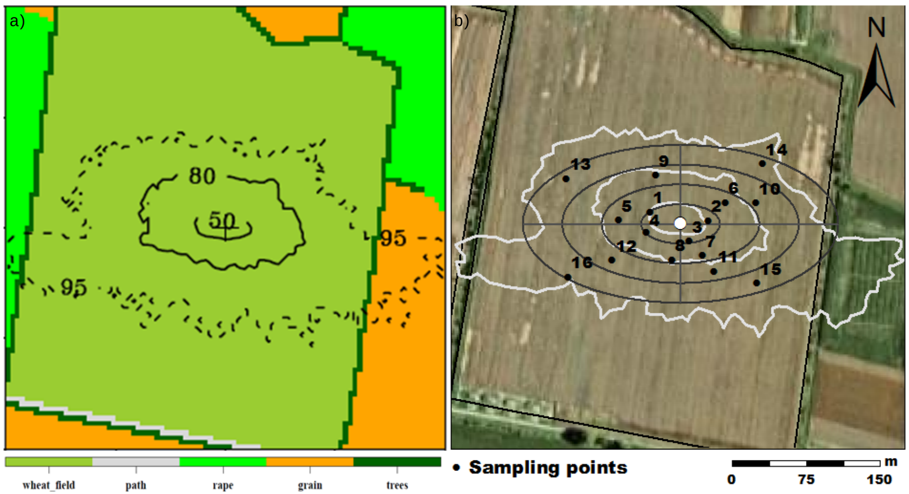

Figure 2. (a) Footprint of the eddy covariance station EC 3 in 2012. Black isolines indicate the fraction of the source area of 50, 80 and 95 % of measured EC fluxes. **(b)** Positions of sampling points within the footprint of EC3 used to measure soil water storage.

BGD
12, 6783–6820, 2015

Energy balance closure on a winter wheat stand

K. Imukova et al.

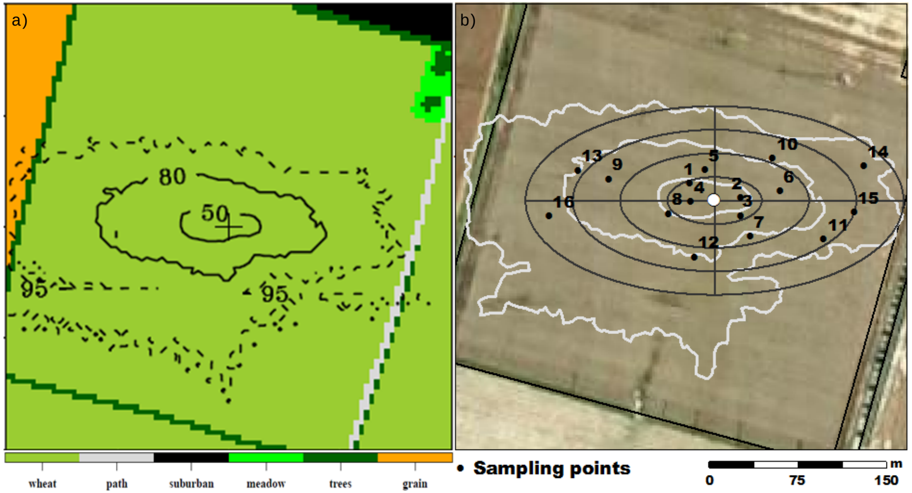

Figure 3. (a) Footprint of the eddy covariance station EC 1 in 2013. Black isolines indicate the fraction of the source area of 50, 80 and 95 % of measured EC fluxes. **(b)** Positions of sampling points within the footprint of EC3 used to measure soil water storage.

cc BY

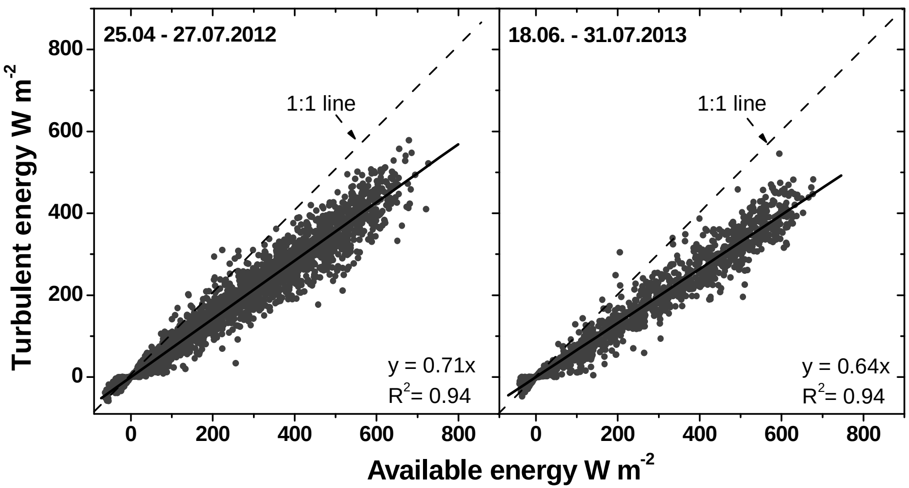

Figure 4. Scatter plots and linear regressions between turbulent and available energy in the periods from April to July 2012 and 2013. The 1 : 1 line indicates perfect energy balance closure.

BGD

12, 6783–6820, 2015

Energy balance closure on a winter wheat stand

K. Imukova et al.

Title Page
Abstract Introduction
Conclusions References
Tables Figures
◂ ▸
Back Close
Full Screen / Esc
Printer-friendly Version
Interactive Discussion

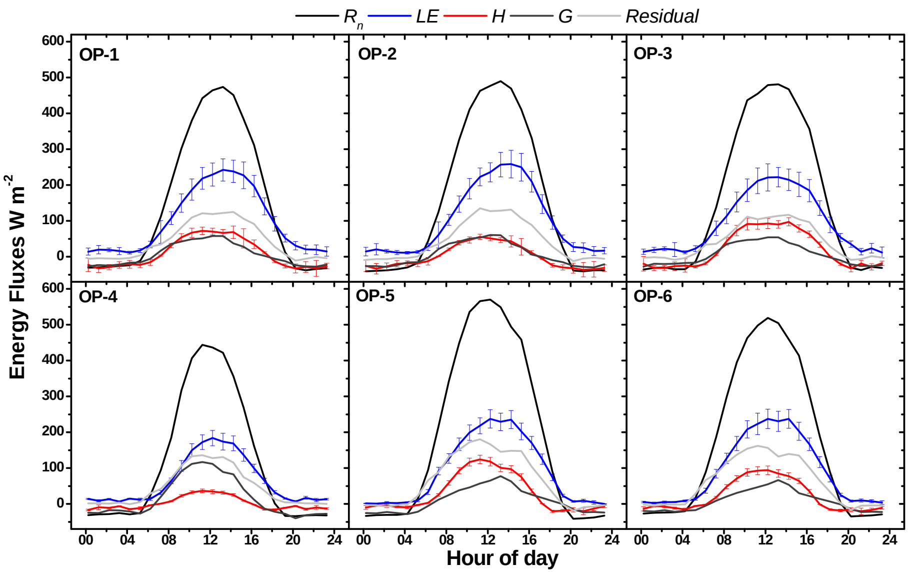

Figure 5. Averaged diurnal cycles of net radiation R_n, latent LE, sensible H and ground heat fluxes G in the observation periods (OPs) of 2012 (OP 1–3) and 2013 (OP 4–6).

BGD
12, 6783–6820, 2015

cc BY

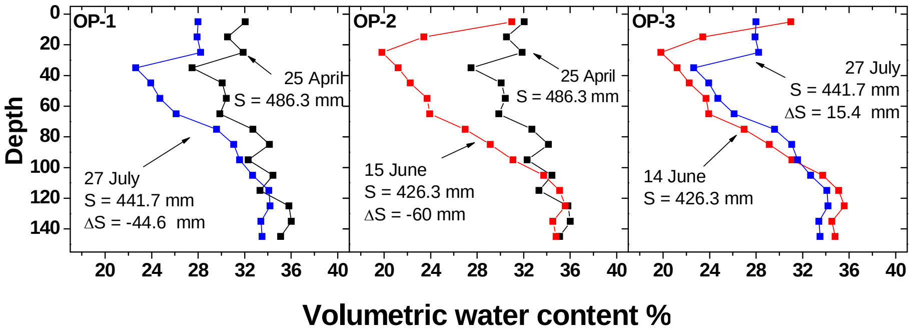

Figure 6. Vertical soil water profiles and change in water storage over three observation periods (OPs) at winter wheat stands at EC3 in 2012.

BGD
12, 6783–6820, 2015

Energy balance closure on a winter wheat stand

K. Imukova et al.

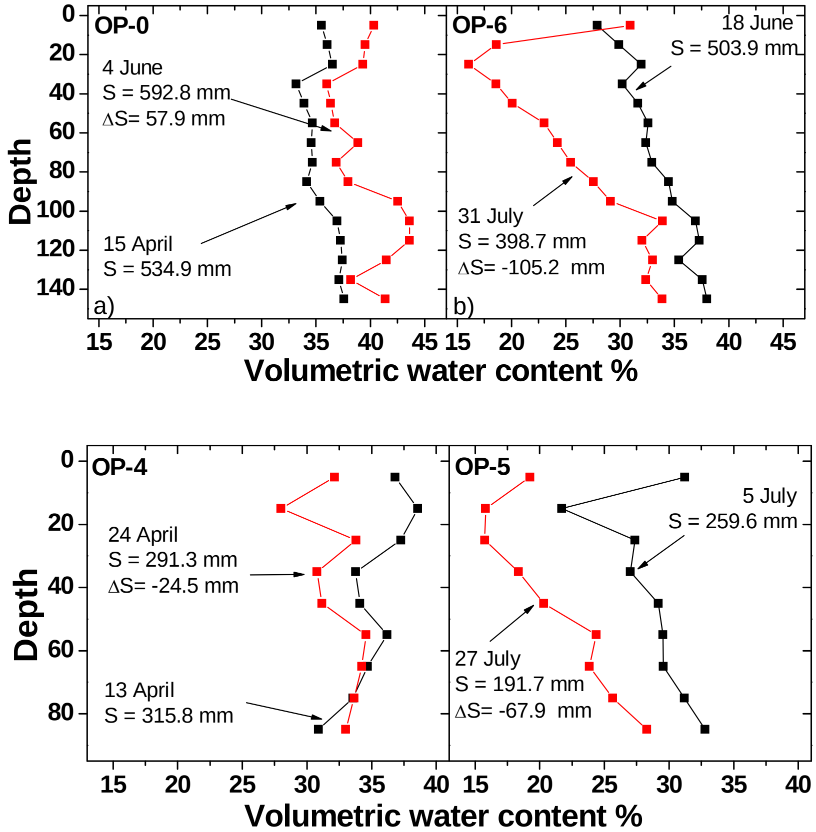

Figure 7. Vertical soil water profiles and change in water storage over four observation periods (OPs) at winter wheat stands at EC1 in 2013. The upper row shows the results of the soil sample campaigns. The soil water contents measured with capacitance soil moisture probes (SM1, Adcon Telemetry, Austria) are shown in the lower row.

BGD
12, 6783–6820, 2015

CC BY

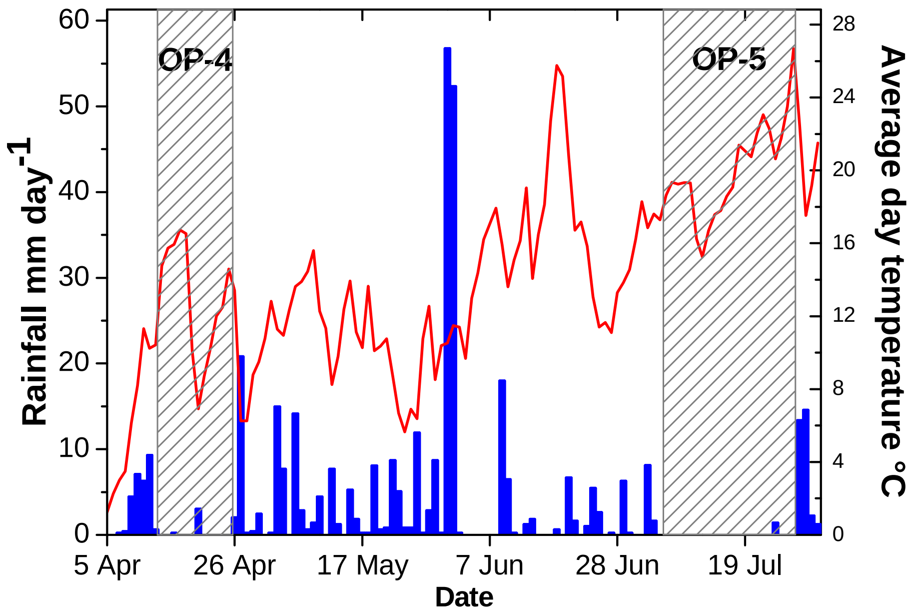

Figure 8. Diurnal rainfall and mean temperature during the 2013 vegetation period. Hatched zones (OP-4, OP-5) indicate periods with low amount of rain and seepage.

BGD

12, 6783–6820, 2015

Energy balance closure on a winter wheat stand

K. Imukova et al.

CC BY

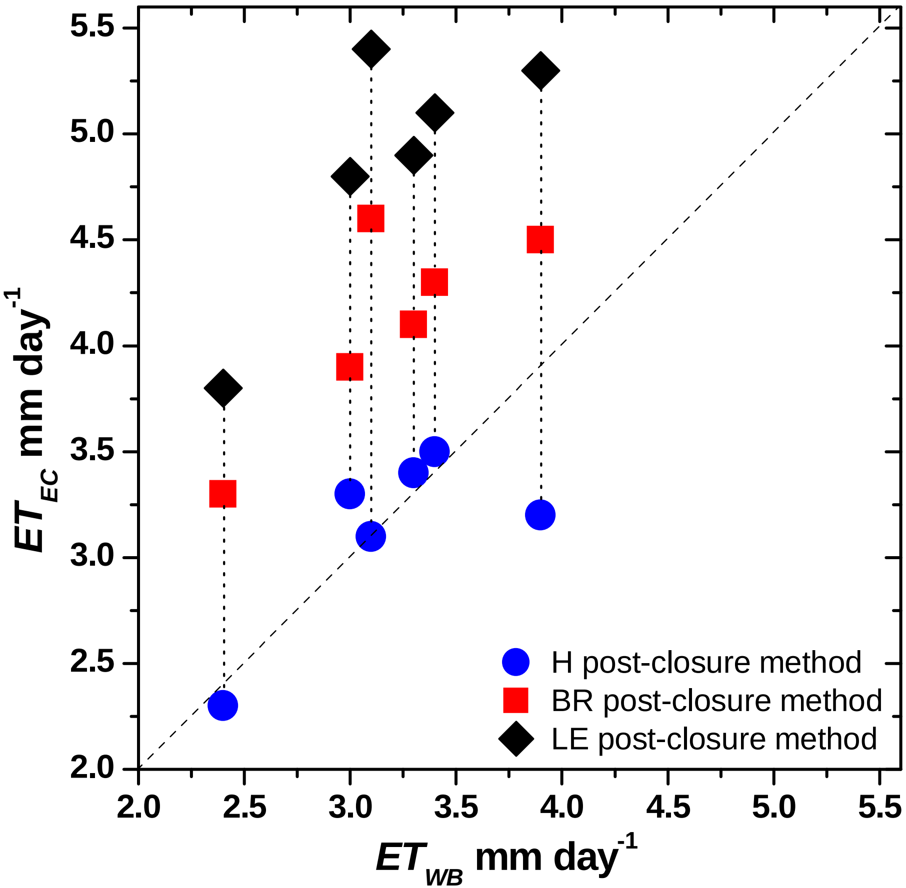

Figure 9. Scatter plots between evapotranspiration assessed from the soil water balance, ET_{WB}, and evapotranspiration measured by the eddy covariance technique, ET_{EC}, adjusted by the sensible heat flux (H), the Bowen ratio (BR) and the latent heat flux (LE) post-closure method.

BGD
12, 6783–6820, 2015

Energy balance closure on a winter wheat stand

K. Imukova et al.

CC BY